Adaptive piezoelectric metacomposite: a new integrated technology to control vibroacoustic power flow

Manuel Collet, Morvan Ouisse, Mohamed Ichchou, Flaviano Tateo, Tianly Huang

ACOUSTICS 2012

Adaptive piezoelectric metacomposite: a new integrated technology to control vibroacoustic power flow

M. Collet[a], M. Ouisse[a], M. Ichchou[b], F. Tateo[a] and T. Huang[b]

[a]Département de Mécanique Appliquée R. Chaléat, 24 chemin de l'Epitaphe - 25000 Besançon
[b]Laboratoire de Tribologie et Dynamique des Systèmes, 36 Avenue Guy de Collongue, 69134 Ecully Cedex
manuel.collet@univ-fcomte.fr

In this paper, we present an application of the Floquet-Bloch theorem in the context of electrodynamics for vibroacoustic power flow optimization by mean of distributed and shunted piezoelectric patches. The main purpose of this work is first to propose a dedicated numerical approach able to compute the multi-modal wave dispersions curves into the whole first Brillouin zone for periodically distributed 2D shunted piezo-mechanical systems. By using two specific indicators evaluating the evanescent part of Bloch's waves and the induced electronic damping, we optimize the piezoelectric shunting electrical impedance for controlling energy diffusion into the proposed semi-active distributed set of cells. Sound radiation efficiency is also analyzed for showing the effects of such smart metamaterial for controlling acoustical noise.

1 Introduction

Tailoring the dynamical behavior of wave-guide structures can provide an efficient and physically elegant means to optimize mechanical components with regards to vibration and acoustic criteria, among others. However, achieving this objective may lead to different outcomes depending on the context of the optimization. In the preliminary stages of a product's development, one mainly needs optimization tools capable of rapidly providing global design direction. Such optimization will also depend on the frequency range of interest. One usually discriminates between the low frequency (LF) range and the medium frequency (MF) range, especially if vibration and noise are considered. However, it should be noted that LF optimization of vibration is more common in the literature than MF optimization. For example, piezoelectric materials and other adaptive and smart systems are employed to improve the vibroacoustic quality of structural components, especially in the LF range. Recently, much effort has been spent on developing new multi-functional structures integrating electro-mechanical systems in order to optimize their vibroacoustic behavior over a larger frequency band of interest[1, 2, 3, 4, 5]. However, there is still a lack of studies in the literature for MF optimization of structural vibration. To that end, the focus of this study is to provide a suitable numerical tool for computing wave dispersion in 2D periodic systems incorporating controlling electronics devices. The final aim is to allow their optimization in order to optimize vibroacoustic diffusion in 2D wave guides and analyze its effect on acoustic radiation [6, 7].

After recalling the Floquet-Bloch theorems, we introduce a new numerical formulation for computing the multi-modal damped wave numbers dispersion in the whole first Brillouin domain of a periodical smart structure made of periodically distributed shunted piezoelectric patches. Based on this wave modeling, optimization of the electrical impedance of the shunted circuit is performed in order to decrease the group velocity of flexural waves or to increase damping induced by the electric circuit. The obtained optimal impedances are also tested in controlling the MF response of a semi-distributed infinite system.

2 Piezo-elasto-dynamical application of the Floquet-Bloch theorem

In this section the application of the celebrated Floquet-Bloch theorem is presented for piezo-elastodynamic problems. Based on the well known results obtained by Floquet [8] in one-dimensional and later rediscovered by Bloch [9] in multidimensional problems, we propose an original application to bi-dimensional piezo-elastodynamical problem leading to very general numerical implementation for computing waves dispersion for periodically smart distributed mechanical systems incorporating electronic components and damping effects [10].

2.1 The Bloch Theorem

The Bloch theorem gives the form of homogeneous states of Schrödinger equation with periodic potential. This theorem can be considered as a multidimensionnal application of the Floquet theorem. The periodic medium properties satisfy a periodic condition as $M(\boldsymbol{x}+R.\boldsymbol{m}) = M(\boldsymbol{x})$, $\boldsymbol{m} \in \mathbb{Z}^3$ where $R = [\boldsymbol{r}_1, \boldsymbol{r}_2, \boldsymbol{r}_3] \in \mathbb{R}^{3\times3}$ is a matrix grouping the three lattice's basis vectors (in 3D). We can also define the primitive cell as a convex polyhedron of $\mathbb{R}^3$ called Ω_x. The reciprocal unit cell is denoted by Ω_k limited by the reciprocal lattice vector defined by the three vectors $\boldsymbol{g}_j$ so that: $\boldsymbol{r}_i.\boldsymbol{g}_j = 2\pi\delta_{ij}$ ($\delta_{i,j}$ being the Kronecker index). We note $G = [\boldsymbol{g}_1, \boldsymbol{g}_2, \boldsymbol{g}_3]$ the reciprocal lattice matrix in the later. If Ω_x is the irreductible primitive cell, Ω_k corresponds to the first Brillouin zone of the lattice.

The Bloch Theorem stipulates that any functions $\boldsymbol{u}(\boldsymbol{x}) \in L^2(\mathbb{R}^3, \mathbb{C}^n)$ can be expressed as

$$\boldsymbol{u}(\boldsymbol{x}) = \int_{\Omega_k} e^{i\boldsymbol{k}\boldsymbol{x}} \tilde{\boldsymbol{u}}(\boldsymbol{x}, \boldsymbol{k}) d\boldsymbol{k} \tag{1}$$

where the Bloch amplitude $\tilde{\boldsymbol{u}}(\boldsymbol{x}, \boldsymbol{k})$ is Ω_x-periodic and has the representations

$$\begin{aligned} \tilde{\boldsymbol{u}}(\boldsymbol{x}, \boldsymbol{k}) &= \sum_{\boldsymbol{n}\in\mathbb{Z}^3} \hat{\boldsymbol{u}}(\boldsymbol{k} + G\boldsymbol{n}) e^{iG\boldsymbol{n}.\boldsymbol{x}}, \\ \boldsymbol{u}(\boldsymbol{x}) &= \frac{|\Omega_x|}{(2\pi)^3} \sum_{\boldsymbol{n}\in\mathbb{Z}^3} \boldsymbol{u}(\boldsymbol{x} + R\boldsymbol{n}) e^{i\boldsymbol{k}(\boldsymbol{x}+R\boldsymbol{n})} \end{aligned} \tag{2}$$

where $\hat{\boldsymbol{u}}(\boldsymbol{k})$ stands for the Fourier transform of $\boldsymbol{u}(\boldsymbol{x})$. One can also demonstrate that the mean value of the Bloch amplitude is the Fourier amplitude of $\boldsymbol{u}(\boldsymbol{x})$ for the corresponding wave vector: $\langle \tilde{\boldsymbol{u}}(., \boldsymbol{k}) \rangle_{\Omega_x} = \hat{\boldsymbol{u}}(\boldsymbol{k})$. Using the Bloch theorem to represent the solutions of periodical partial derivative equations implies that all derivatives are shifted by $\boldsymbol{k}$ in the sense given by the used spatial operator.

Based on that theorem one can define the expansion functions $\boldsymbol{v}_m(\boldsymbol{x}, \boldsymbol{k})$, called the Bloch eigen modes, such that they can be used to represent the Bloch amplitudes of any solution of the corresponding partial derivative equation as

$$\tilde{\boldsymbol{u}}(\boldsymbol{x}, \boldsymbol{k}) = \sum_m \boldsymbol{u}_m(\boldsymbol{k}) \boldsymbol{v}_m(\boldsymbol{x}, \boldsymbol{k}) \tag{3}$$

and at the same time diagonalize the partial derivative equations. One notes that the expansion coefficients $\boldsymbol{u}_m(\boldsymbol{k})$ depend on the applied disturbance and also on the induced wave vector (see [11] for details).

2.2 Application to Piezo-Elastodynamic

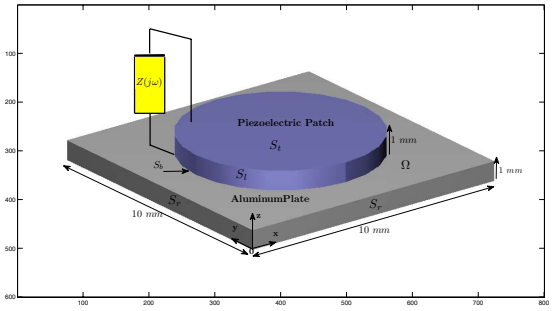

Figure 1: Generic 3D piezocomposite periodic cell

Let us consider a piezo-elastodynamic problem made of infinite periodic distribution of unitary cell described in figure 1. The harmonic homogeneous dynamical equilibrium of system is driven by the following partial derivative equation:

$$\begin{cases} \rho\ddot{\boldsymbol{w}}(\boldsymbol{x}) - \nabla\sigma(\boldsymbol{x}) = 0 & \forall \boldsymbol{x} \in \Omega_x \\ -\nabla D(\boldsymbol{x}) = 0 & \forall x \in \Omega_x \end{cases} \tag{4}$$

where $\boldsymbol{w}(\boldsymbol{x}) \in \mathbb{R}^3(\Omega_x)$ is the displacement vector, σ represents the Cauchy stress tensor, $\epsilon = \nabla_{sym} w = \frac{1}{2}(\nabla w^T(x) + w(x)\nabla^T)$ the Green strain tensor, $D(\boldsymbol{x})$ the electric displacement. The linear constitutive material behavior relationships can be written as

$$\sigma = C_E(\boldsymbol{x})\epsilon - e^T(\boldsymbol{x})\boldsymbol{E} \tag{5}$$
$$\boldsymbol{D} = e(\boldsymbol{x})\epsilon + \varepsilon_S(\boldsymbol{x})\boldsymbol{E} \tag{6}$$

where $\boldsymbol{E} = -\nabla V$ the electric field vector (V the voltage), C_E the elasticity tensor at constant electrical field, e^T the piezoelectric coupling tensor and ε_S the dielectric permittivity at constant strain. We add to this set of equilibrium equations an output expression

$$q^o = -\int_{S_t} \boldsymbol{D}.\boldsymbol{n} dS \tag{7}$$

allowing the introduction of the charge measurement on the piezoelectric's top electrode and hence the dual counterpart of the imposed electrical Dirichlet boundary condition for applying the shunt impedance operator.
The equations above are consistent for each kind of material to the extent that null piezoelectric and permittivity tensors can be used when passive materials are considered. All of these tensors also depend on the spatial location vector $\boldsymbol{x}$. The piezo-elastodynamic equilibrium can also be written as: $\forall \boldsymbol{x} \in \Omega_x$

$$\rho\omega^2\boldsymbol{w}(\boldsymbol{x}) + \nabla C\nabla_{sym}(\boldsymbol{w}(\boldsymbol{x})) + \nabla e^T(\boldsymbol{x})\nabla V(\boldsymbol{x}) = 0 \tag{8}$$
$$-\nabla e(x)\nabla_{sym}(\boldsymbol{w}(\boldsymbol{x})) + \nabla\varepsilon_S(x)\nabla V(\boldsymbol{x}) = 0 \tag{9}$$

As the problem is 2D infinitely periodic, only electrostatic boundary conditions have to be considered on each cell:

$$\begin{cases} V = 0 & \forall x \in S_b \\ V = V^o & \forall x \in S_t \\ \boldsymbol{D}.\boldsymbol{n} = 0 & \forall x \in S_l \end{cases} \tag{10}$$

where S_b is the grounded bottom electrode of the piezoelectric layer, S_t is the top electrode connected to the external shunt and s_l the lateral electrode less boundary. The top electrode applied feedback voltage V_o depends on the shunt characteristic and on the collected charges q^o (7) and can be expressed in the Fourier space by:

$$V^o(i\omega) = -Z(i\omega)q^o(i\omega) \tag{11}$$

By considering a primitive cell of the periodic problem Ω_x and by using the Bloch theorem, we can compute the associated Bloch eigenmodes (3) and the dispersion functions by searching the eigen solutions of the homogeneous problem (8) and (9) as:

$$\boldsymbol{u}(\boldsymbol{x}) = \begin{bmatrix} \boldsymbol{w}(\boldsymbol{x}) \\ V(\boldsymbol{x}) \end{bmatrix} = \boldsymbol{u}_{n,k}(\boldsymbol{x})e^{i\boldsymbol{k}.\boldsymbol{x}} \tag{12}$$

with $\boldsymbol{u}_{n,k}(\boldsymbol{x}) = \begin{bmatrix} \boldsymbol{w}_{n,k}(\boldsymbol{x}) \\ V_{n,k}(\boldsymbol{x}) \end{bmatrix}$, Ω_x periodic functions. By introducing expression (12) in the piezo-elastodynamic equations (8), (9), one can demonstrate that $\boldsymbol{w}_{n,k}(\boldsymbol{x})$, $V_{n,k}(\boldsymbol{x})$ and $\omega_n(\boldsymbol{k})$ are solutions of the generalized eigenvalues problem:

$$\begin{aligned} 0 &= \rho\omega_n^2(\boldsymbol{k})\boldsymbol{w}_{n,k}(\boldsymbol{x}) + \nabla C\nabla_{sym}(\boldsymbol{w}_{n,k}(\boldsymbol{x})) \\ &+ ik\left\{(C\nabla_{sym}(\boldsymbol{w}_{n,k}(\boldsymbol{x}))).\boldsymbol{\Phi}\right. \\ &+ \nabla(C\Xi_{n,k}(\boldsymbol{x}))\} - k^2(C\Xi_{n,k}(\boldsymbol{x}))).\boldsymbol{\Phi} \\ &+ \nabla e^T\nabla V_{n,k}(\boldsymbol{x}) + ik\left\{(\nabla e^T V_{n,k}(\boldsymbol{x})).\boldsymbol{\Phi}\right. \\ &+ \left.(e^T\nabla V_{n,k}(\boldsymbol{x})).\boldsymbol{\Phi}\right\} \\ &- k^2 V_{n,k}(\boldsymbol{x})(e^T\boldsymbol{\Phi}).\boldsymbol{\Phi}\ \forall \boldsymbol{x} \in \Omega_x \end{aligned} \tag{13}$$

$$\begin{aligned} 0 &= -\nabla e\nabla_{sym}(\boldsymbol{w}_{n,k}(\boldsymbol{x})) - ik\left\{\nabla(e\Xi_{n,k}(\boldsymbol{x}))\right. \\ &\quad \left.+(e\nabla_{sym}(\boldsymbol{w}_{n,k}(\boldsymbol{x}))).\boldsymbol{\Phi}\right\} \\ &+ k^2(e\Xi_{n,k}(\boldsymbol{x})).\boldsymbol{\Phi} \\ &+ \nabla\varepsilon_S\nabla V_{n,k}(\boldsymbol{x}) + ik\left\{(\nabla\varepsilon_S V_{n,k}(\boldsymbol{x})).\boldsymbol{\Phi}\right. \\ &+ \left.(\varepsilon_S\nabla V_{n,k})(\boldsymbol{x}).\boldsymbol{\Phi}\right\} \\ &- k^2(\varepsilon_S\boldsymbol{\Phi}V_{n,k}(\boldsymbol{x})).\boldsymbol{\Phi}\ \forall \boldsymbol{x} \in \Omega_x \end{aligned} \tag{14}$$

with the associated boundary conditions:

$$\begin{cases} \boldsymbol{w}_{n,k}(\boldsymbol{x} - R.\boldsymbol{m}) = \boldsymbol{w}_{n,k}(\boldsymbol{x}) & \forall \boldsymbol{x} \in S_r\ \boldsymbol{m} \in \mathbb{Z}^2 \\ V_{n,k}(\boldsymbol{x}) = 0 & \forall \boldsymbol{x} \in S_b \\ V_{n,k}(\boldsymbol{x})V = -Z(i\omega)q^o_{n,k} & \forall \boldsymbol{x} \in S_t \\ \boldsymbol{D}.\boldsymbol{n} = 0 & \forall \boldsymbol{x} \in S_l \end{cases} \tag{15}$$

where $\boldsymbol{k} = k\begin{bmatrix} cos(\phi) \\ sin(\phi) \\ 0 \end{bmatrix} = k\boldsymbol{\Phi}$ where ϕ represents the direction angle into the reciprocal 2D lattice domain and $\Xi_{n,k}(\boldsymbol{x}) = \frac{1}{2}(\boldsymbol{w}_{n,k}(\boldsymbol{x}).\Phi^T + \Phi.\boldsymbol{w}^T_{n,k}(\boldsymbol{x}))$ the symmetric dyadic tensor or the dyadic product of the displacement $\boldsymbol{w}_{n,k}(\boldsymbol{x})$ and direction vector Φ. S_r are the interface of the cells continuum, and R the matrix grouping the two lattice's basis vectors (in 2D in the considered problem). In the electrical boundary conditions, $q^o_{n,k}$ is given by:

$$\begin{aligned} q^o_{n,k} &= \int_{S_t}[-e(\nabla_{sym}(\boldsymbol{w}_{n,k}(\boldsymbol{x})) + ik\nabla e\Xi_{n,k}(\boldsymbol{x})) \\ &+ \varepsilon_S(\nabla V_{n,k}(\boldsymbol{x}) + ikV_{n,k}(\boldsymbol{x})\boldsymbol{\Phi}].\boldsymbol{n}dS \end{aligned} \tag{16}$$

where $\boldsymbol{n}$ is the outpointing unitary normal vector.
The proposed formulation is also based on the computation of the Floquet vectors (13), (14), instead of computing the Floquet propagators commonly used for elastodynamic applications. Our approach allows to obtain the full 2D waves dispersions functions and to clearly introduce damping and electrical impedance into the piezo-elastodynamic operator. The adopted methodology allows the computation of the complete complex map of the dispersion curves including evanescent waves and allowing the introduction of damping and shunt operator if any.

2.3 Numerical Computation of the Bloch's waves

The numerical implementation is obtained by using a standard finite elements method to discretized the weak formulation of equations (13), (14). The assembled matrix equation is also given by:

$$\begin{aligned} 0 &= (K(Z(i\omega_n(\lambda,\phi)) + \lambda L(\phi, Z(i\omega_n(\lambda,\phi))) \\ &- \lambda^2 H(\phi, Z(i\omega_n(\lambda,\phi))) - \omega_n^2(\lambda,\phi)M)\boldsymbol{u}_{n,k}(\phi), \quad (17) \end{aligned}$$

where $\lambda = ik$, M and $K(Z(i\omega_n(\lambda,\phi)))$ are respectively the standard symmetric semi-definite mass and stiffness matrices (the mass matrix is semi definite because elastostatic equation are condensed into the equation), $L(\phi, Z(i\omega_n(\lambda,\phi)))$ is a skew-symmetric matrix and $H(\phi, Z(i\omega_n(\lambda,\phi)))$ is a symmetric semi-definite positive matrix.

When k and ϕ are fixed and Z does not depend on ω the system (17) is a linear eigen value problem allowing us to compute the dispersion functions $\omega_n^2(\boldsymbol{k},\phi)$ and the associated Bloch eigenvector $\boldsymbol{u}_{n,k}(\phi)$.

If a highly damped system (K, L, H are complex frequency dependent) and a frequency dependent electrical shunt impedance are considered, the obtained eigenvalue problem is not quadratic and a complex specific numerical methodology has to be implemented. Furthermore, evanescent part of propagating waves appear as the imaginary part of eigenfrequencies. It then becomes very difficult to distinguish the propagative and evanescent waves as all solution appear complex. Another much more suitable possibility for computing dispersion in damped systems, dedicated for time/space deconvolution and for computation of diffusion properties as defined by [1, 12], is to consider the following generalized eigen value problem:

$$\begin{aligned} 0 &= (K(Z(\omega) - \omega^2 M + \lambda_n(\omega,\phi)L(\phi, Z(\omega)) \\ &- \lambda_n^2(\omega,\phi)H(\phi, Z(\omega)))\boldsymbol{u}_n(\omega,\phi). \quad (18) \end{aligned}$$

In this problem, the pulsation ω is a real parameter corresponding to the harmonic frequency. Wave's numbers and Floquet vectors are then computed. An inverse Fourier transformation in the k-space domain can lead us to evaluate the physical wave's displacements and energy diffusion operator when the periodic distribution is connected to another system as in [1]. As L is skew-symmetric, the obtained eigen values are quadruple $(\lambda, \bar{\lambda}, -\lambda, -\bar{\lambda})$ collapsing into real or imaginary pairs (or a single zero) when all matrices are real (i.e. for an undamped system). In this case a real pair of eigen values correspond to evanescent modes oriented in two opposite directions on the k-space and imaginary values to two traveling waves propagating in opposite direction.

As previously mentioned, the real part of $\boldsymbol{k} = k\boldsymbol{\Phi}$ vector is restricted to stand inside the first Brillouin zone. In the quadratic eigen value problem (18) nothing restricts computation to only find eigen values satisfying this condition. For direction vector $\boldsymbol{\Phi}$ orthogonal to the lattice facelets, the periodical conditions expressed for one dimensional wave guide are still valid: if $\lambda_j(\omega, \boldsymbol{\Phi}_p)$ is an eigen value associated to $\boldsymbol{w}_j(\omega, \boldsymbol{\Phi}_p)$ then $\forall \boldsymbol{m} \in \mathbb{Z}^3$, $\lambda + i.\boldsymbol{\Phi}_p^T(G.\boldsymbol{m})$ is also an eigen value associated to $\boldsymbol{w}_j(\omega, \boldsymbol{\Phi}_p)e^{-i.\boldsymbol{\Phi}_p^T(G.\boldsymbol{m})x}$. Thus, for undamped systems, all obtained eigenvalues are periodically distributed in the $\boldsymbol{k}$-space along its principal directions.

2.4 Computation of the evanescence and damped power flow criteria

One aim of this paper is to provide a numerical methodology for optimizing the piezoelectric shunt impedance $Z(\omega)$ for controlling energy flow into the periodically distributed piezo-composite structure. For doing this, we need to define suitable criteria.

The first used criterion is based on the computation of the waves group velocities. Indeed, they indicate how energy is transported into the considered system and allow to distinguish the 'propagative' and 'evanescent' waves. If one Bloch eigen solution (i.e $\boldsymbol{u}_n(\omega,\phi)$, $k_n(\omega)$) is considered, the associated group velocity vector [13] is given by:

$$\boldsymbol{C}_{g_n}(\omega,\phi) = \nabla_{\boldsymbol{k}}\omega = \frac{\langle\langle \boldsymbol{S} \rangle\rangle}{\langle\langle e_{tot} \rangle\rangle} = \frac{\langle \boldsymbol{I} \rangle}{\langle E_{tot} \rangle} \quad (19)$$

where $\langle\langle : \rangle\rangle$ is the spatial and time average respectivelly on one cell and one period, $\boldsymbol{S}$ is the density of energy flux defined in [13], $\boldsymbol{I}$ the mean intensity and e_{tot}, E_{tot} the total piezomechanical energy and its time average on a period (see [13] for details). In this problem, we only consider mechanical energy transportation as the electrostatic coupling is decentralized and can be condensed as a mechanical interface as proved in [14] and generally computed in [15]. So we also compute the intensity vector $\boldsymbol{I}$ by:

$$\langle \boldsymbol{I}_n \rangle(\omega,\phi) = -\frac{\omega}{2V_{ol}} Re\left(\int_{\Omega_x} C(\varepsilon_n(\boldsymbol{x}) + ik\Xi_n(\boldsymbol{x})).(\boldsymbol{w}_n^*(\boldsymbol{x}))\right) d\Omega \quad (20)$$

where $.^*$ is the complex conjugate and V_{ol} the domain volume. As the spatio-temporal average of the system Lagragian is null (see [13]), the total energy average is approximated by only computing the kinetic energy average:

$$\langle E_{tot} \rangle(\omega,\phi) = \frac{1}{2V_{ol}} Re\left(\int_{\Omega_x} \rho\omega^2 \boldsymbol{w}_n(\boldsymbol{x}).\boldsymbol{w}_n^*(\boldsymbol{x}i) d\Omega\right) \quad (21)$$

The group velocity vectors $\boldsymbol{C}_{g_n}(\omega,\phi)$ is computed for all wave numbers at each frequency. In order to focus our analysis on only flexural modes (S and SH ones) we introduce an indicator allowing to select them by computing the ratio of kinetic energy average on out of plane displacement as:

$$Ind(n,\omega,\phi) = \frac{\frac{1}{2V_{ol}}\left(\int_{\Omega_x} \rho\omega^2 wz_n(\boldsymbol{x}) wz_n^*(\boldsymbol{x}) d\Omega\right)}{\langle E_{tot} \rangle} \quad (22)$$

Piezoelectric Material		
Symbol	Value	Property
$s^E_{11} = s^E_{22} = s^E_{33}$	$11.6e^{-12}\ Pa^{-1}$	compliance matrix
$s^E_{12} = s^E_{13} = s^E_{23}$	$-3.33e^{-12}\ Pa^{-1}$	compliance matrix
$s^E_{44} = s^E_{55} = s^E_{66}$	$45.0e^{-11}\ Pa^{-1}$	compliance matrix
η	0.1 %	Hysteretic Damping ratio
$d_{31} = d_{32}$	$-6e^{-11}\ C/N$	piezoelectric matrix
d_{33}	$15.2e^{-11}\ C/N$	piezoelectric matrix
$d_{24} = d_{15}$	$730e^{-12}\ C/N$	piezoelectric matrix
ρ	$7600kg/m^3$	Density
$\varepsilon^T_{11} = \varepsilon^T_{22}$	$504.1\ \varepsilon_o\ C/V/m$	Dielectric Permittivity
ε^T_{33}	$270\ \varepsilon_o\ C/V/m$	Dielectric Permittivity

Table 1: *Piezoelectric patch characteristics*

with $wz_n(\boldsymbol{x}, \omega, \phi)$ being the (Oz) component of vector $\boldsymbol{w}_n(\boldsymbol{x}, \omega, \phi)$. Optimization of the shunt impedance $Z(i\omega)$ is based on the minimization of the maximum group velocity collinear to the wave number vector (19) for waves having a ratio of transported flexural kinetic energy (22) greater than 0.8. The used criterion can also be written as:

$$Crit_1(Z(i\omega), \phi) = max_{n/Ind(n,\omega,\phi)>0.8}(\boldsymbol{C}_{g_n}(\omega, \phi).\boldsymbol{\Phi}) \qquad (23)$$

The second used criterion is based on the maximization of the damped electric power directly express as the active electrical power $P_{elec}(n, \omega, \phi) = \frac{1}{2} real(i\omega Z(i\omega) q^o_{n,k} q^{o*}_{n,k})$. If one wants to increase damping effect inside the smart metamaterial, this term need to be sufficiently large. In the second case, the used criteria is also

$$Crit_2(Z(i\omega), \phi) = max_{n/Ind(n,\omega,\phi)>0.8} \frac{1}{P_{elec}(n, \omega, \phi)} \qquad (24)$$

3 Optimization of the Flexural energy flow inside the shunted periodic piezo-composite

The considered piezo-composite cell is presented in figure 1. The supporting plate material is standard aluminum with 0.1 % of hysteretic damping ratio and the piezoelectric material characteristics are given in table 1.

The used numerical optimizations of the criteria are based on a multidimensional unconstrained nonlinear minimization (Nelder-Mead).

3.1 Optimization of the waves goupes velocities by using $Crit_1$

In a first test, we optimize the waves groups velocities by using $Crit_1$ given in equation (23).

It can be immediately observed that the optimization of the shunt impedance leads to a large decrease of the group velocity of the A_0 mode while the A_1 wave, which becomes propagative at 8.8 kHz, is not controlled by the optimal configuration (see figure 2). The bending waves also propagate energy with a very slow velocity and can be considered as evanescent. Flexural energy is, also, only transported by the A_1 mode after the cutting frequency.

The real and imaginary parts of the optimal impedance are plotted in figure 3 for all angles ϕ. The optimal impedance values almost correspond to a constant

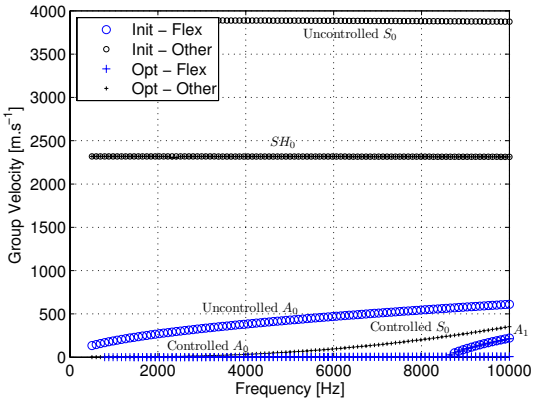

Figure 2: Group velocities along (Ox) direction. o: initial value of shunt; +: optimal value of shunt. Large marks correspond to flexural waves, small marks correspond to other waves

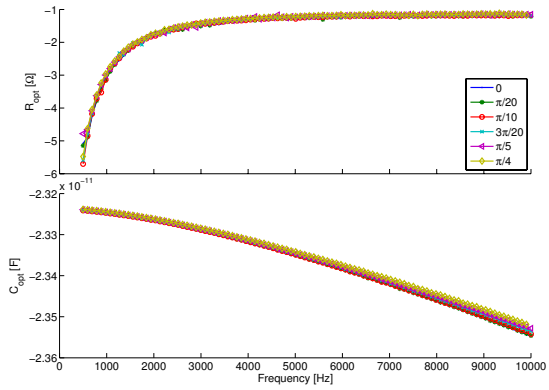

Figure 3: Optimal electric impedance, represented as equivalent resistance and capacitance, obtained along 6 direction forming an angle with (Ox) axis of $\frac{n\pi}{20}$ with n being all integers from 0 to 5.

negative capacitance in all directions. The corresponding average value is $-233.66\ pC.V^{-1}$. Equivalent resistances corresponding to the active part of the shunt impedance (figure 3) are negative which indicates that the optimization leads to provide energy to the system for controlling mechanical damping effects introduced by hysteretic terms in the model. The optimized configuration also tends to converge towards a fully conservative system. The obtained mean value of the resistance is $-1.5319\ \Omega$. This is confirmed in figure 4 where the electrical dissipated energy appears negative when the optimal shunt is connected to the patch. This observation is one of the main issue of this work.

In order to check this point, an optimization run has been performed on a highly damped system, using an hysteretic coefficient of 5 %. The optimized configurations leads to a behaviour which is very similar to results obtained with lower structural damping value. It can be underlined that the electric circuit is fully active with smaller negative resistive parts of average value $-74.88\ \Omega$. The observed proportionality between the optimal average resistances (-1.5319 and $-74.88\ \Omega$) and the chosen mechanical damping terms (0.1 % and 5 %) indicates that the optimization leads to annihilate mechanical damping in order to reach a total cancellation of the group velocity of A_0 mode. The final controlled system is then almost fully

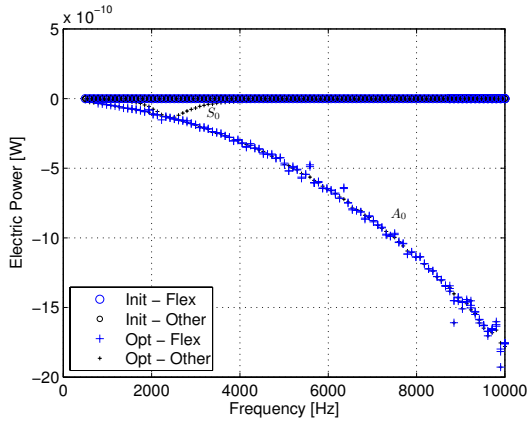

Figure 4: Damped power inside the electric circuit. o: initial value of shunt; +: optimal value of shunt. Large marks correspond to flexural waves, small marks correspond to other waves

reactive.

3.2 Optimization of damped power flow inside the electric shunts by using $Crit_2$

In this second test, we optimize the damped power flow inside the electric shunts by using $Crit_2$ given in equation (24). The group velocities of propagative waves along (Ox) are presented in figure 6, while the real and imaginary parts of the optimal impedance are plotted in figure 8 and the electrically damped power in figure 7.

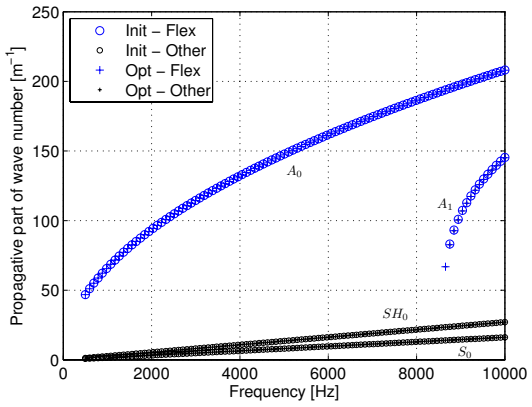

Figure 5: Propagative parts of the wave number $kx_n(i\omega)$ along (Ox), for hysteretic damping of 3 % (only propagating waves included). o: initial value of shunt; +: optimal value of shunt. Large marks correspond to flexural waves, small marks correspond to other waves

The optimal impedances of the electric shunts are plotted in figure 8 for various values of ϕ.

The first observation is that the optimization of the shunt impedance for improving the absorption characteristics of the system induces modifications of the group velocities of the controlled waves (see figure 6), while the propagative part of the wave numbers remain unchanged (figure 5). This can be explained by a large improvement of the ratio between the real and imaginary parts of the waves numbers, which physically corresponds to the forcing of propagating effects to increase damping effects: energy can propagate

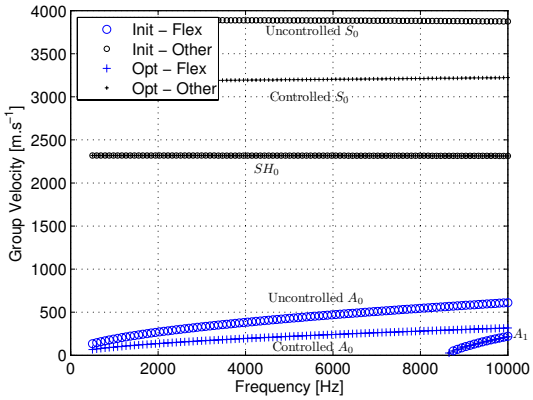

Figure 6: Group velocities along (Ox) direction. o: initial value of shunt; +: optimal value of shunt. Large marks correspond to flexural waves, small marks correspond to other waves

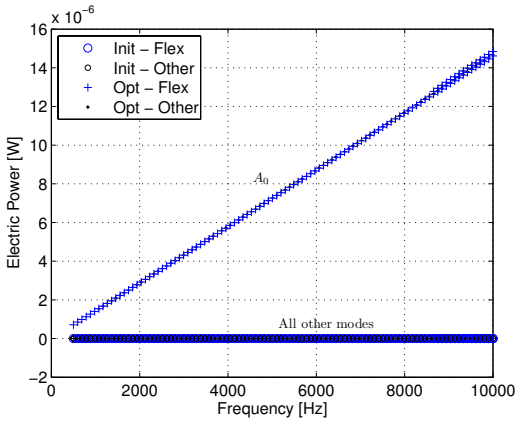

Figure 7: Damped power inside the electric circuit. o: initial value of shunt; +: optimal value of shunt. Large marks correspond to flexural waves, small marks correspond to other waves

inside the periodically distributed set of active cells for allowing electrical energy conversion. The figure 7 shows that a the dissipated power is largely increased when optimal shunt is connected to the patch.

The optimal impedance values correspond to an almost constant negative capacitance in all directions (see figure 8). The corresponding average value is $-237.43\ pC.V^{-1}$. Equivalent resistances corresponding to the active part of the shunt impedance (figure 8) are positive, which is in accordance with the fact that a damping effect is awaited.

4 Conclusions

This paper presents a numerical procedure able to compute the damped wave's dispersion functions in the whole first Brillouin domain of multi dimensionnal piezo-elastodynamical wave guides. The method was applied for determining the optimal impedance allowing to minimize the group velocities of the flexural waves. Based on this approach, some numerical tests on a finite dimension system incorporating a semi-distributed set of shunted piezo-composite cells have been performed. We underline a strong influence of the designed shunt circuits in the

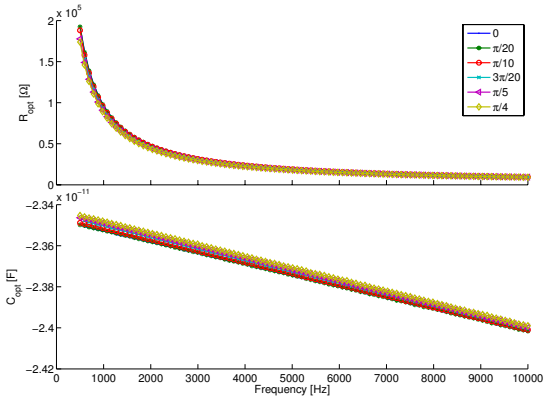

Figure 8: Optimal electric impedance, represented as equivalent resistances and capacitances, obtained along 6 direction forming an angle with (Ox) axis of $\frac{n\pi}{20}$ with n being all integers from 0 to 5.

dynamical response of the system and the coupled noise radiation. Even if the link between the obtained wave properties are not clearly established, we also demonstrated that our developed numerical procedures can be used for optimizing the energy diffusion operator of such adaptive mechanical interface. To do so, additional work has to be done for optimizing the complete interface scattering and for controlling the evanescent waves playing an important role in the dynamical response of a finite system incorporating such semi-distributed interface. Another part of this future developments should deal with the complete vibroacoustic optimization incorporating a fully fluid-structure coupling effect.

The proposed methodology can also be used for studying particular dissipation phenomenon such as those induced by complex shunted piezoelectric patches as proposed by [16], or even foams or complex polymers behaviors. The proposed method furnishes an efficient tool for future optimization of distributed smart cells as proposed in the case of 1D wave guide by [1].

Acknowledgments

This work was carried out with a grant of French agency ANR number $NT09-617542$. We gratefully acknowledge the French ANR and CNRS for supporting this program.

References

[1] M. Collet, K. Cunefare, and N. Ichchou, "Wave Motion Optimization in Periodically Distributed Shunted Piezocomposite Beam Structures," *Journal of Int Mat Syst and Struct*, vol. 20, no. 7, pp. 787–808, 2009.

[2] O. Thorp, M. Ruzzene, and A. Baz, "Attenuation and localization of wave propagation in rods with periodic shunted piezoelectric patches," *Proceedings of SPIE - The International Society for Optical Engineering Smart Structures and Materials*, vol. 4331, pp. 218–238, 2001.

[3] B. Beck, K. A. Cunefare, M. Ruzzene, and M. Collet, "Experimental analysis of a cantilever beam with a shunted piezoelectric periodic array," in *ASME-SMASIS*, (Philadelphia), ASME, Sept 28 Oct 1 2010.

[4] I. Bartoli, A. Marzani, F. L. di Scalea, and E. Viola, "Modeling wave propagation in damped waveguides of arbitrary cross-section," *Journal of Sound and Vibration*, vol. 295, pp. 685–707, AUG 22 2006.

[5] M. Foda, A. Almajed, and M. ElMadany, "Vibration suppression of composite laminated beams using distributed piezoelectric patches," *Smart Materials and Structures*, vol. 19, no. 11, p. 115018, 2010.

[6] M. Collet, M. Ouisse, M. Ruzzene, and M. Ichchou, "A Floquet-Bloch decomposition of the elastodynamical equations: application to bi-dimensional wave's dispersion computation of damped mechanical system.," *International Journal of Solids and Structures*, vol. In press, 2011.

[7] M. Collet, M. Ouisse, M. Ichchou, and M. Ruzzene, "Semi-active optimization of 2d waves dispersion into mechanical systems by the mean of periodically distributed shunted piezoelectric patches: a new class of adaptive metamaterials,," in *SPIE Smart Structures/NDE, San-Diego (CA)*, 2011.

[8] G. Floquet, "Sur les équations différentielles linéaires á coefficients périodiques," *Annales de l'Ecole Normale Supérieure*, vol. 12, pp. 47–88, 1883.

[9] F. Bloch, "Über die Quantenmechanik der Electron in Kristallgittern," *Zeitschrift für Physik*, vol. 52, pp. 550–600, 1928.

[10] M. Collet, M. Ouisse, M. Ichchou, and M. Ruzzene, "Numerical tools for semi-active optimization of 2d waves dispersion into mechanical system," in *ASME-SMASIS*, (Philadelphia), ASME, Sept 28 Oct 1 2010.

[11] A. Bensoussan, J. Lions, and G. Pananicolaou, *Asymptotic Analysis for Periodic Structures*. North Holland, 1978.

[12] J. Mencik and M. Ichchou, "Multi-mode propagation and diffusion in structures through finite elements," *European Journal of Mechanics A-Solids*, vol. 24, no. 5, pp. 877–898, 2005.

[13] W. Maysenhölder, *Körperschall-energie Grundlagen zur Berechnung von Energiedichten und Intensitäten*. Wissenschaftliche Verlagsgesellschaft, Stuttgart, 1994.

[14] N. W. Hagood and A. H. von Flotow, "Damping of structural vibrations with piezoelectric materials and passive electrical networks," *Journal of Sound and Vibration*, vol. 146(2), pp. 243–268, 1991.

[15] M. Collet and K. Cunefare, "Modal Synthesis and Dynamical Condensation Methods for Accurate Piezoelectric Systems Impedance Computation," *Journal of Int Mat Syst and Struct*, vol. 19, no. 11, pp. 1251–1271, 2008.

[16] F. Casadei, M. Ruzzene, B. Beck, and K. Cunefare, "Vibration control of plates featuring periodic arrays of hybrid shunted piezoelectric patches," in *Proceedings of SPIE - Smart Structures and Materials*, vol. 7288, SPIE, 2009.